CHAPTER 3
A 1D MODEL OF THE FREEZE LINING AND FURNACE WALL

This chapter describes the details of a dynamic one-dimensional model of the furnace freeze lining and wall. The development process followed during this modelling effort closely resembles the process described by Thomas and Brimacombe (1997). The same development process was used for the models discussed in following two chapters.

The model described in this chapter was used to build a more comprehensive process model (see CHAPTER 5, page 89) and in the execution of experiments to investigate phenomena related to the freeze lining (see CHAPTER 6, page 137; and CHAPTER 7, page 176).

3.1 IDENTIFICATION

The model being described in this chapter is identified as follows:

Name: Freeze Lining Conductor Model

Abbreviation: FLC Model

3.2 PROBLEM DEFINITION

The main objective of this study was to investigate the dynamic interaction between the freeze lining and slag bath in an ilmenite-smelting furnace. For this reason it was necessary to develop a mathematical model of the freeze lining that can describe its behaviour as a function of time. This was the most basic requirement.

The behaviour of the freeze lining that was of interest includes changes in thickness, composition and temperature as functions of time, and, in the case of composition and temperature, as functions of position in the freeze lining.

Because both slag bath temperature and composition are known to have an important influence on the behaviour of the freeze lining (Pistorius, 1999), the model had to be able to address both these aspects.

3.3 SYSTEM DESCRIPTION

Before becoming involved with the details of phenomena and mathematics relevant to the model, it is necessary to first gain perspective about the physical system to be modelled. For this reason the reader is referred back to the simplified schematic representation of an ilmenite-smelting furnace (Figure 8, page 13).

The schematic shows a sectional view of a circular DC electric arc furnace with a single hollow electrode. Feed is introduced into the furnace through the hollow electrode. Metal and slag are tapped from the furnace through separate tap holes.

For the FLC model, the region including the freeze lining and furnace wall is of particular importance. This region is shown in somewhat more detail below:

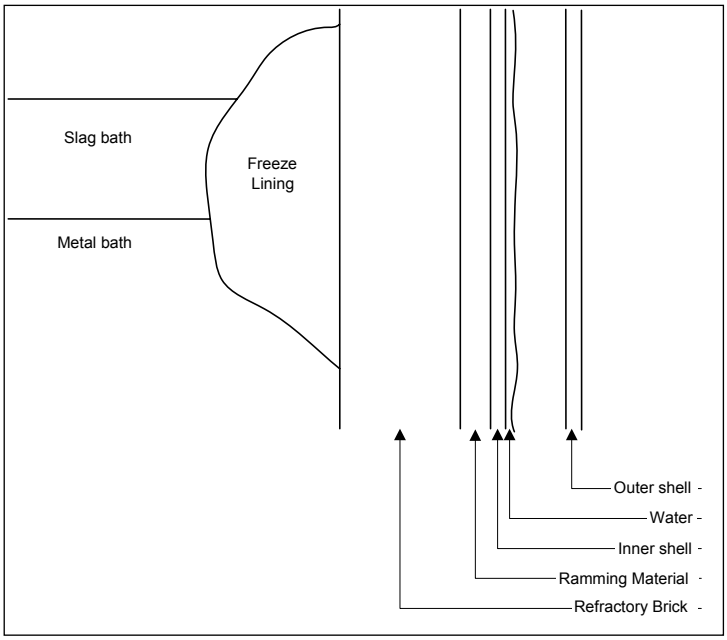

Figure 16 – Schematic representation of the freeze lining and wall region of the furnace.

3.3.1 System geometry

If one only focuses on the part of the furnace shown in Figure 16, the system to be modelled is cylindrical. For this reason, phenomena occurring in the furnace will be identified and described based on the cylindrical coordinate system and therefore the following geometrical dimensions:

- Radial dimension
- Axial dimension
- Angular dimension

3.4 KEY PHENOMENA

To be able to model a process, one needs to be aware of all or most of the phenomena that are active in the process. For this reason, the next few paragraphs aim to identify most of the phenomena that are relevant to the system being considered in this chapter. It also aims to classify these phenomena in terms of their importance to the FLC model.

3.4.1 Heat Transfer

a. Radial heat transfer

Outward radial heat transfer is the direction of heat transfer that is of primary concern in the system. The reason is that the electric arc is the main source of energy in the furnace. The arc discharges a significant portion of its energy into the slag bath (Stenkvist and Bowman, 1987). The slag bath then transfers, via conduction and convection, heat to the metal bath and freeze lining. It also radiates heat into the furnace atmosphere (Reynolds, 2002).

Focusing on the system being considered here, energy will flow

- through the slag bath by means of conduction and convection,

- from the slag bath to the freeze lining by convection,
- through the freeze lining, refractory materials and steel inner shell by conduction, and
- into the cooling water on the outer surface of the inner shell by convection.

Radial heat transfer, including all the components listed above, was seen as a key phenomenon since modelling of this phenomenon is crucial to the usefulness of the FLC model. This is because solidification and melting of the freeze lining move the interface between the freeze lining and slag bath primarily in the radial dimension.

b. Axial heat transfer

Because of the slag bath being the hottest part in the furnace other than the arc itself, heat flows away from it to regions of lower temperature. Heat is transferred via convection and radiation to the furnace atmosphere and by convection to the metal bath. The metal bath and furnace atmosphere can therefore be safely assumed to have lower temperatures than the slag bath. Due to this it is very likely that there is an axial heat transfer component in the system being considered.

There is likely to be upward transfer of heat in the furnace wall from the region of the slag bath towards the colder upper sidewall regions. It is also possible that there is downward heat transfer in the sidewall towards the colder lower sidewall regions that are in contact with liquid metal. The likelihood that liquid metal in these regions are in direct contact with the refractory lining (with no freeze lining) could however result in a much higher temperature boundary condition compared with the region of the sidewall that is in contact with the freeze lining. This will result in an upward axial heat transfer component from the level of the metal bath.

It is believed that the magnitude of axial components of heat transfer vectors within the system is significantly smaller than the radial components. Due to this, axial heat transfer was seen as being less important than radial heat transfer (Assumption 3.1, page 35). It was not believed to be a key phenomenon within the context of the FLC model.

c. Angular heat transfer

Due to the cylindrical shape of the furnace, it is convenient to assume symmetry about the cylinder's central axis in terms of freeze lining thickness, temperature, etc. However, because of the presence of tap holes on the side of the furnace, and the likelihood of the electrode (and therefore the arc) being off-centre, this symmetry does not exist in reality. For this reason temperature, freeze lining thickness and even freeze lining composition should vary with angular position.

It is believed that the magnitude of angular components of heat transfer vectors within the system is significantly smaller than the radial components. Due to this, angular heat transfer was seen as being less important than radial heat transfer (Assumption 3.1, page 35). It was not believed to be a key phenomenon within the context of the FLC model.

d. Heat sources

The following known heat sources are found in the system or influence the system as boundary conditions:

- Electric arc

  The electric arc heats the furnace atmosphere, slag bath and metal bath directly. This heat reaches the freeze lining via convection and conduction. Heat can also be radiated to the freeze lining in the case when slag or metal tapping exposes part of the freeze lining to the arc.

  This heat source was seen as key to the FLC model.

- Slag solidification

  When slag solidifies on the surface of the refractory bricks or the freeze lining heat associated with the phase change is liberated.

  This heat source was seen as key to the FLC model because the liberated heat must be accounted for in a heat transfer model of the furnace wall and freeze lining. Ignoring it would have resulted in a serious weakness in the model.

- Chemical reaction

  Various chemical reactions (to be discussed in more detail below) can occur in the system. Some of these reactions are exothermic and therefore act as heat sources.

  This heat source was seen as key to the FLC model for reasons similar to those quoted for the heat liberated during slag solidification.

e. Heat sinks

The following known heat sinks are found in the system or influence the system as boundary conditions:

- Slag melting

  When material melts away on the surface of the refractory bricks or the freeze lining, heat associated with the phase change is absorbed.

  This heat sink was seen as key to the FLC model for the same reasons as the slag solidification heat source.

- Chemical reaction

  Various chemical reactions (to be discussed in more detail below) can occur in the system. Some of these reactions are endothermic and therefore act as heat sinks.

  This heat sink was seen as key to the FLC model for the same reasons as the slag solidification heat source.

- Water cooling

  Forced water cooling is applied on the outer surface of the inner steel shell. The water extracts heat as it exits the system.

  This heat sink was seen as important to the FLC model, but since the extraction of heat by water cooling is not the rate-determining step in heat transfer from the slag bath to the water, it was

decided not to model this phenomenon in great detail. A simple boundary condition assumption was used to describe this heat sink (Assumption 3.8, page 38).

3.4.2 Mass Transfer

a. Convective mass transfer

Due to movement in the slag and metal baths that is induced by the impinging arc, entering feed material, electromagnetic forces and buoyancy forces, material (slag and metal) is transported to and from the freeze lining surface and the refractory brick surface (if some refractory material is exposed to the slag and metal baths).

Convective mass transfer was not seen as a critical/key phenomenon to the FLC model. The reason is that it was assumed that the slag bath is well mixed due to the momentum transferred to it by the above-mentioned forces (Assumption 4.2, page 36).

b. Diffusion

Due to compositional gradients inside the metal and slag baths it is expected that diffusion occurs in these zones.

Compositional gradients can also exist in the freeze lining due to slag of different compositions having solidified at different positions. Such gradients also induce diffusion.

Diffusion was not seen as a critical/key phenomenon to the FLC model. The reason for this was again the strong stirring effects that are present in the metal and slag baths. In the case of the freeze lining it was simply assumed that mass transfer does not have a significant impact on the behaviour of the freeze lining (Assumption 3.3, page 36). Ideal mixing in the liquid, with no diffusion in the solid, corresponds to the assumptions of the Scheil model of solidification (Flemings, 1997).

3.4.3 Momentum Transfer

a. Slag and metal baths

Momentum is transferred to the slag bath by the impinging arc, material fed through the centre of the electrode, and by electromagnetic and buoyancy forces. This results in movement in the slag and metal baths. This movement can influence the rates at which heat and mass are transferred to and from the freeze lining.

Momentum transfer in the slag bath was seen as an important phenomenon for the FLC model since it can significantly influence heat transfer at the freeze lining surface. This phenomenon therefore had to be addressed in the model. It was however believed that it would be adequate to incorporate this phenomenon as a simple boundary condition without modelling it in any great detail.

b. Water-cooling layer

Water flows down the outer surface of the inner shell (see Figure 16, page 28) under the influence of gravity. This momentum transfer influences the rate at which heat is extracted by the water from the wall.

Momentum transfer in the water cooling layer was not seen as a key phenomenon for the FLC model. The heat transfer resulting from it was believed to be important, but since it is not rate-determining, it could be addressed adequately by a simplifying assumption regarding this heat transfer boundary condition (Assumption 3.8, page 38).

3.4.4 Chemical Reaction

a. Reaction between liquid slag and liquid slag

It is likely that some chemical reactions may take place in the liquid slag. For example Fe_2O_3 may be reduced by Ti_2O_3 to form FeO and TiO_2.

Since the slag bath acts as a boundary condition to the heat transfer FLC model and because the calculations of solidification and melting influence liquid slag composition, these reactions were seen as important to the FLC model.

b. Reaction between liquid slag and solid slag

Due to strong mixing in the slag bath and the compositional variations of the slag bath with time, liquid slag coming into contact with the freeze lining will often differ in composition from the solid material of the freeze lining. Solidification by itself enriches the liquid phase in certain species resulting in a compositional difference between the solid and liquid phases at the interface between the freeze lining and slag bath. The combination of the difference in composition, the difference in phase (liquid versus solid) and likely difference in temperature could often result in a chemical potential difference/gradient between the liquid slag close to the freeze lining and the freeze lining itself. Such a gradient acts as the driving force for chemical reaction between slag bath and freeze lining. In this case chemical reaction refers to reaction between species in the same phases, between species in different phases and changes from one phase to another (for example liquid and solid phases).

These chemical reactions were seen as a critical part of the behaviour of the system since it occurs at the interface between the slag bath and freeze lining. Describing the movement of this interface in response to process changes was partly the aim of this modelling study, and these chemical reactions therefore had to be modelled.

c. Reaction between solid slag and solid slag

Compositional variations may occur in the freeze lining as a function of radial position. This may be due to variations in slag bath composition. These compositional variances can result in chemical potential gradients that provide a driving force for chemical reactions to take place.

Such chemical reactions were assumed to be negligible for the purpose of the FLC model (Assumption 3.3, page 36). In the solid state, the reaction rates and mass transfer rates are likely to be slow. For this reason the inaccuracies that result from the assumption were accepted.

d. Reaction between slag and refractory material

It was uncertain whether any significant reaction takes place at the interface between the freeze lining (solid slag) and the refractory material. It was expected that chemical reaction at this interface will not be important to the overall accuracy of the model since it should occur at very low rates.

If the freeze lining is completely dissolved into the slag bath, liquid slag will come into contact with refractory material. The reaction between liquid slag and refractory material becomes important in this situation. Since the aim in practice is to prevent the entire freeze lining from melting away, chemical reaction between liquid slag and refractory material is a limiting condition. For this reason it was not seen as key to the FLC modelling exercise. A complete loss of freeze lining in the FLC model can be considered indicative of refractory erosion.

3.4.5 Mechanical Effects

a. Tapping equipment

Tapping equipment (drills, lances and clay guns) can significantly influence the behaviour of the freeze lining in the vicinity of the tap holes. The focus of this study was however not on these regions, and these mechanical effects were not seen as important to the accuracy of the FLC model. They were therefore ignored.

b. Buoyancy in the metal bath

Due to the lower density of solid slag (approximately 3,800 kg/m^3) compared with liquid metal (approximately 7,000 kg/m^3), the freeze lining will experience upward buoyancy forces from below when it becomes partially submerged in the metal bath. This effect was however not the focus of the FLC model and was ignored.

3.4.6 Summary of Key Phenomena

The table below summarises the phenomena identified above and assigns a level of importance to each phenomenon within the context of the FLC model. A level of importance of 1 means that the phenomenon is considered unimportant and it is subsequently ignored. Level 2 indicates that the phenomenon must be incorporated into the model, but it is not necessary to model it in detail. Level 3 marks critical phenomena that must be modelled in as much detail as possible.

			Level of importance to current modelling effort		
			1	2	3
Heat transfer	Radial	In slag bath		✔	
		Slag bath to freeze lining			✔
		In freeze lining			✔
		Freeze lining to refractory brick			✔
		In refractory brick			✔
		Refractory brick to ramming material			✔
		In ramming material			✔
		Ramming material to steel shell			✔
		In steel shell			✔
		Steel shell to water		✔	
	Axial	In slag bath	✔		
		In freeze lining	✔		

		In refractory brick	✔				
		In ramming material	✔				
		In steel shell	✔				
		In water	✔				
	Angular	In slag bath	✔				
		In freeze lining	✔				
		In refractory brick	✔				
		In ramming material	✔				
		In steel shell	✔				
		In water	✔				
	Heat sources	Electric arc					✔
		Slag solidification					✔
		Chemical reaction					✔
	Heat sinks	Slag melting					✔
		Chemical reaction					✔
		Water cooling				✔	
Mass transfer	Convection	In slag bath	✔				
	Diffusion	In slag bath	✔				
		In freeze lining	✔				
Momentum transfer	Slag bath					✔	
	Metal bath		✔				
	Water cooling layer		✔				
Chemical reaction	Liquid slag	With liquid slag	✔				
	Liquid slag	With solid slag					✔
	Liquid slag	With refractory material	✔				
	Solid slag	With solid slag	✔				
	Solid slag	With refractory material	✔				
Mechanical effects	Tapping equipment		✔				
	Buoyancy in metal bath		✔				

Table 2 – Summary of key phenomena for the FLC model.

3.5 APPROACH AND MODEL COMPLEXITY

From the table summarising key phenomena it can be concluded that radial heat transfer, heat sources and sinks, and chemical reaction are of greatest importance to the FLC model. Among these the heat-related phenomena are most basic to the problem being studied. The reason is that the thermal phenomena occur right throughout the system while significant chemical reactions only occur in the slag bath, freeze lining, and perhaps on the hot face of the refractory brick.

Due to the general importance of heat-related phenomena in the system, heat transfer was used as the foundation of the model. The chemical reactions were modelled within the heat transfer framework where applicable.

3.5.1 Modelling of Heat Transfer

Because axial and angular heat transfer were assumed to be of significantly lesser importance than radial heat transfer, and because this model was the first attempt at building a mathematical representation of the system, it was decided to model heat transfer in the radial dimension only. The model is therefore one-dimensional with the radial dimension being labelled the 'focus dimension'.

The axial position in the furnace that was used for the model is one where liquid slag is found all of the time. The influence of liquid metal and the furnace atmosphere on the freeze lining was therefore ignored.

The angular position that was used is one that is representative of most of the circumference of the furnace. This means that the influence of tap holes was ignored in the FLC model.

The range of the radial dimension that was used starts at some distance away from the inner surface of the refractory wall into the slag bath. It ends at the outer surface of the inner steel shell where it is water-cooled. The distance that the model's radial dimension extends into the slag bath was chosen in such a way that there was sufficient room for the interface between the slag bath and freeze lining to move (by solidification and melting) to achieve the desired experimental results.

a. Solution method

A finite difference method was used to solve the heat transfer problem. An explicit formulation was used.

3.5.2 Modelling of Chemical Reaction

In the case of the freeze lining and the slag bath, a complete thermochemical representation of the nodes was maintained in addition to the heat transfer representation. This made it possible to calculate chemical reaction and phase changes by using a Gibbs-free-energy-minimisation approach. This approach simplified modelling of chemical reaction, because one does not need to focus on specific reactions that occur. The Gibbs-free-energy minimiser (Eriksson and Rosen, 1973; Eriksson, 1975) simply searches for the relevant thermodynamic equilibrium condition.

This approach implicitly assumes a strong drive towards thermodynamic equilibrium at the interface between the slag bath and freeze lining (Assumption 3.4, page 36).

3.6 MODEL FORMULATION

3.6.1 Assumptions

The following paragraphs list assumptions made as part of the FLC model formulation. The paragraphs clarify why the assumptions were made, their validity and the impact that the assumptions have on the model.

a. Assumption 3.1

Statement: Axial and angular heat transfer components are negligible and can be ignored.

Justification: This assumption was required to simplify the model. A one-dimensional model is significantly simpler and more manageable compared with two- and three-dimensional models. The results of the current study may lead to the development of such more detailed models if the additional modelling effort is justified by the perceived value that could be added.

Validity: The assumption is certainly not absolutely true since the existence of axial and angular heat transfer components can easily be proven. It is however true that the radial heat transfer components should be significantly larger than the axial and angular components. The assumption was therefore acceptable given the objectives of the current work. The most significant influence on the validity of this assumption is

probably the axial heat transfer component from the portion of the wall in direct contact with the metal bath.

Impact: This assumption causes inaccuracies in the predictions of the model. These inaccuracies were in general viewed as being in balance with other uncertainties (measurement inaccuracies, uncertainty about dimensions, and uncertainty about material properties) in the process, and they were therefore viewed as not being significant within the context of the FLC model and its current application.

b. Assumption 3.2

Statement: The slag bath is well mixed and can therefore be treated as ideally mixed.

Justification: This assumption was required to simplify the model. Taking compositional and thermal variations in the slag bath into account would have complicated the model significantly.

Validity: The assumption is surely not absolutely true, but since there is significant stirring in the slag bath, it could be seen as being valid within the context of the FLC model.

Impact: The impact of this assumption on the accuracy and validity of the model was believed to be minimal.

c. Assumption 3.3

Statement: Mass transfer and solid-state chemical reaction in the freeze lining are negligible and can be ignored.

Justification: This assumption was required to simplify the model. Incorporating mass transfer and chemical reaction between solid nodes with different compositions into the model would have complicated matters significantly. It was uncertain whether it would have added much to the accuracy and validity of the model.

Validity: If compositional gradients exist, mass transfer will occur and chemical reaction is also likely to occur. Because the solid state is being considered here, mass transfer and chemical reactions are likely to be slow relative to other phenomena being modelled. This made the assumption acceptable, even though it is not absolutely true.

Impact: The impact of this assumption on the accuracy and validity of the model was believed to be minimal.

d. Assumption 3.4

Statement: There is a strong drive towards thermodynamic equilibrium at the interface between the slag bath and freeze lining.

Justification: This assumption was required to simplify the modelling of chemical reactions and phase changes at the interface between the slag bath and freeze lining. This assumption made it possible to use a Gibbs-free-energy-minimisation approach to model these reactions.

Validity: Ultimately the tendency towards thermodynamic equilibrium drives all chemical reactions. In some instances this influence is less dominant because of a significant influence of mass transfer, heat transfer and reaction kinetics. In the case being considered here, it was believed that the high temperatures and strong mixing of the

slag bath prevent mass transfer and reaction kinetics from being limiting. Heat transfer plays a significant role and for this reason it was modelled in detail.

Impact: If mass transfer or reaction kinetics plays a significant role in the behaviour of the freeze lining, this assumption would result in noteworthy inaccuracies in the model. This was, however, not believed to be the case.

e. Assumption 3.5

Statement: The temperature dependence of the density of materials (liquid slag, solid slag, magnesia brick, ramming material, and steel) used in this model is negligible and can be ignored.

Justification: This assumption was required to simplify the model. Variations in density with changing temperature result in changes in the volume of the finite-difference nodes used in the model. To properly address such volume changes one needs to use a finite element approach. This would have complicated the model significantly.

Validity: Since it is known that the density of most materials vary with temperature, this assumption is not true. Within the context of the FLC model, it was believed that the inaccuracies introduced by this assumption were within the general uncertainties that are associated with the smelting process. The assumption could therefore be tolerated.

Impact: The assumption introduces inaccuracies into the model, but these were believed to be tolerable.

f. Assumption 3.6

Statement: The thermal conductivity of solid slag is assumed to be 0.001 kW/(m.°C), and independent of temperature.

Justification: No detailed information on thermal conductivity of liquid and solid slag as a function of temperature and/or composition was available for this study.

Validity: The only information regarding the thermal conductivity of high-titania slag in literature was found in the form of an assumption made by Pistorius (2004), and discussions with Pistorius (2004b). The same value used in that work is used here.

Impact: The assumption introduces inaccuracies into the model, but these were believed to be acceptable given the objectives of this study and the availability of thermal conductivity data.

g. Assumption 3.7

Statement: No liquid metal reaches the freeze lining.

Justification: This assumption was required to simplify the FLC model. If this assumption were omitted, the model would have to be constructed to allow liquid metal to enter into the conductor in addition to liquid slag. This would have added some complications to the model, and these complications were not believed to add significantly to the validity or accuracy of the model.

Validity: Because liquid metal is formed in reduction reactions between slag and reductant particles, it is likely that small liquid metal droplets will be dispersed throughout the slag bath. This makes the assumption false. The amount of metal was however believed to be small, which would improve the validity of the assumption.

Impact: The assumption introduces inaccuracies into the model, but these inaccuracies were believed to be minimal. Contact between liquid metal and slag was modelled in other ways in the overall process modelled discussed later.

h. Assumption 3.8

Statement: The outer surface of the steel shell is at a constant temperature.

Justification: This assumption was required to simplify the FLC model. By assuming a constant temperature boundary condition, all the complexity of the convective water cooling boundary condition was ignored.

Validity: The water cooling boundary condition is not the rate-determining step in the heat transfer path from the freeze lining surface to the water cooling on the outside of the steel shell. The influence of variations in water cooling was also not the focus of this study. For these reasons this assumption was acceptable even though it is not true.

Impact: The assumption introduces inaccuracies into the FLC model but because the water cooling boundary condition is not rate determining, these inaccuracies were believed to be acceptable.

i. Assumption 3.9

Statement: The contact resistances between the layers (solid slag, brick, ramming, steel) of the conductor are not rate-determining of heat transfer through the wall.

Justification: This assumption was required to simplify the FLC model. It is virtually impossible to measure or infer the actual contact resistances in the furnace being considered. For this reason the contact resistances are made as small as possible without causing numerical instabilities in the model.

Validity: Due to significant expansion of refractory brick and ramming when the furnace is brought into operation, it was believed that the mechanical contact between the brick and ramming, and between ramming and steel is very tight with no air gaps of note being present. This would result in these contact resistances having a smaller influence than conduction through the solid slag and brick layers.

The contact between the solid slag and the brick was also believed to be very tight due to the high temperatures experienced during the initial period when the furnace is brought into operation. For this reason this resistance was believed not to be rate-determining.

Impact: The assumption and the subsequent determination of the contact resistances introduced inaccuracies into the FLC model. Because the resistances were made as small as possible and because they are very likely not rate-determining in reality, these inaccuracies were believed to be negligible.

3.6.2 Simplifications

The following paragraph presents a simplification that was made in the model. The justification and impact of the simplification are also presented.

a. Simplification 3.1

Description: The influence of contact between the metal bath and the freeze lining on freeze lining behaviour is ignored.

Justification: This simplification was made to avoid having to treat the details of varying slag and metal bath levels in the model.

Impact: The simplification introduces inaccuracies into the model, but since the influences of tapping on freeze lining behaviour were not set as an objective of this study, it was deemed to be acceptable.

3.6.3 Material Definitions

a. Liquid Slag

Liquid Slag is found in contact with the freeze lining on the inside of the furnace. Because of the interaction between liquid slag and solid slag at this interface, it was required to include the Liquid Slag material into the model.

Liquid Slag is defined to contain only a single liquid phase. This phase is referred to as the Liquid Slag Phase.

The relevant physical properties of this material are given in APPENDIX A.

i. Liquid Slag Phase

Actual constituents: From chemical analyses this phase is known to contain the following constituents: Al_2O_3, CaO, Cr_2O_3, FeO, Fe_2O_3, K_2O, MgO, MnO, Na_2O, P_2O_5, SiO_2, TiO_2, Ti_2O_3, V_2O_3, and ZrO2.

Considered constituents: For the purpose of the FLC model, only the following phase constituents were considered: FeO, Fe_2O_3, TiO_2, and Ti_2O_3.

Solution model: Quasichemical Model (Eriksson et al., 1996)

Thermochemical data: ChemSage format data file from GTT Technologies.

b. Liquid Metal

Liquid Metal can be produced as part of the reactions taking place between liquid slag and solid slag at the interface between the slag bath and the freeze lining.

Liquid Metal is defined to contain only a single liquid phase. This phase is referred to as the Liquid Metal Phase.

The relevant physical properties of this material are given in APPENDIX A.

i. Liquid Metal Phase

Actual constituents: From chemical analyses this phase is known to contain the following constituents: Al, Cr, Fe, Mn, P, Si, Ti, V, C, and O.

Considered constituents: For the purpose of the FLC model, the following phase constituents were considered: Fe, C, O, Ti, TiO, and Ti_2O.

Solution model: Unified Interaction Parameter Formalism (Bale and Pelton, 1997)

Thermochemical data: ChemSage format data file from GTT Technologies.

c. Solid Slag

The freeze lining consists of Solid Slag. Since the freeze lining is the primary consideration of the model, it was necessary to include this material in the model formulation.

Solid Slag is defined to contain the following phases:

- Pseudobrookite Solid Solution Phase
- Rutile Solid Solution Phase

The relevant physical properties of this material are given in APPENDIX A.

i. Pseudobrookite Solid Solution Phase

Actual constituents: It is known (Pistorius and Coetzee, 2003; FactSage 5.2) that the following ions are found in this phase: Ti^{4+}, Ti^{3+}, Cr^{3+}, Al^{3+}, V^{3+}, Fe^{2+}, Mg^{2+}, and Mn^{2+}. They occur in a solid solution. The basic forms of the compounds that make up the solid solution are $M^{2+}(Ti^{4+})_2O_5$ and $(M^{3+})_2OTi^{4+}O_5$.

Considered constituents: For the purpose of the FLC model, only the following phase constituents were considered: $(FeTi_2O_5)^{2-}$, $(Ti_3O_5)^{+}$, $FeTi_2O_5$, and $(Ti_3O_5)^{-}$. (The solution model used to describe this phase is an ionic formalism. For this reason some of the constituents are indicated as being ions rather than neutral species.)

Solution model: 2-Sublattice Ionic Formalism (Eriksson et al., 1996; GTT Technologies 1998)

Thermochemical data: ChemSage format data file from GTT Technologies.

ii. Rutile Solid Solution Phase

Actual constituents: This solid solution can contain the following constituents TiO_2, Ti_2O_3, and ZrO_2 (Eriksson et al., 1996; FactSage 5.2).

Considered constituents: For the purpose of the model being considered in this chapter, only the following phase constituents were considered: TiO_2 and Ti_2O_3.

Solution model: General Polynomial Kohler/Toop Formalism (Eriksson et al., 1996; GTT Technologies, 1998)

Thermochemical data: ChemSage format data file from GTT Technologies.

d. Magnesia Brick

The furnace wall contains magnesia brick on the level of the slag bath. These bricks consist mostly of MgO with minor levels of impurities. Because no chemical reactions were considered where MgO was involved, this material and its phases were viewed in a simplified manner. For this reason impurities such as Fe_2O_3, Al_2O_3, CaO and SiO_2 that are known to be present in the brick, were ignored.

Magnesia Brick is defined to contain only a single phase, named Magnesia Phase.

The relevant physical properties of this material are given in APPENDIX A.

i. Magnesia Phase

Actual constituents: The phases occurring in the Magnesia Brick are known to contain MgO, Fe_2O_3, Al_2O_3, CaO and SiO_2.

Considered constituents: For the purpose of the model being considered in this chapter, the phase is viewed as being pure MgO.

Solution model: None

Thermochemical data: FactSage 5.2. (Bale et al, 2002)

e. Ramming

Ramming is used between the steel shell and the refractory brick on the level of the slag bath. Very little information was available about this material, but it seems to consist of mostly graphite. Because no chemical reactions were considered where Ramming was involved, this material and its phases were viewed in a simplified manner.

Ramming is defined to contain only a single phase, named Graphite Phase.

The relevant physical properties of this material are given in APPENDIX A.

i. Graphite Phase

Actual constituents: Except for graphite, the phases and phase constituents actually occurring in the Ramming was not known.

Considered constituents: For the purpose of the FLC model, the phase was viewed as being pure carbon.

Solution model: None

Thermochemical data: FactSage 5.2. (Bale et al, 2002)

f. Steel

Steel is used for the shell that contains the Ramming, Magnesia Brick and the slag and metal baths. No information was available about this material, but, since it is steel, it could be safely assumed to consist mostly of iron.

Steel is defined to contain only a single phase, named Steel Phase.

i. Steel Phase

Actual constituents:	Except for Fe and C, the phases and phase constituents actually occurring in the Steel were not known.
Considered constituents:	For the purpose of the FLC model, the phase is viewed as consisting of Fe, C and Mn.
Solution model:	Ideal Mixture
Thermochemical data:	FactSage 5.2. (Bale et al, 2002)

3.6.4 Model Structure

The FLC model is primarily a one-dimensional heat transfer model. The final structure of this model is now defined. Because of the confidentiality of actual furnace parameters, the author devised a set of furnace dimensions for use in the current work. It was attempted to choose the dimensions in such a way that the results of this work are relevant to industrial furnace operations.

Heat transfer was modelled by dividing the one-dimensional representation of the region of interest (Figure 17) into layers and the layers into finite-difference nodes. A heat balance was performed on each node during each time step. An explicit finite difference formulation was used.

The following layers were used in the model:

- Freeze Lining (Abbreviated as *FL*. This layer contains both Solid Slag and Liquid Slag material.)
- Brick Layer (Abbreviated as *BL*.)
- Ramming Layer (Abbreviated as *RL*.)
- Steel Layer (Abbreviated as *SL*.)

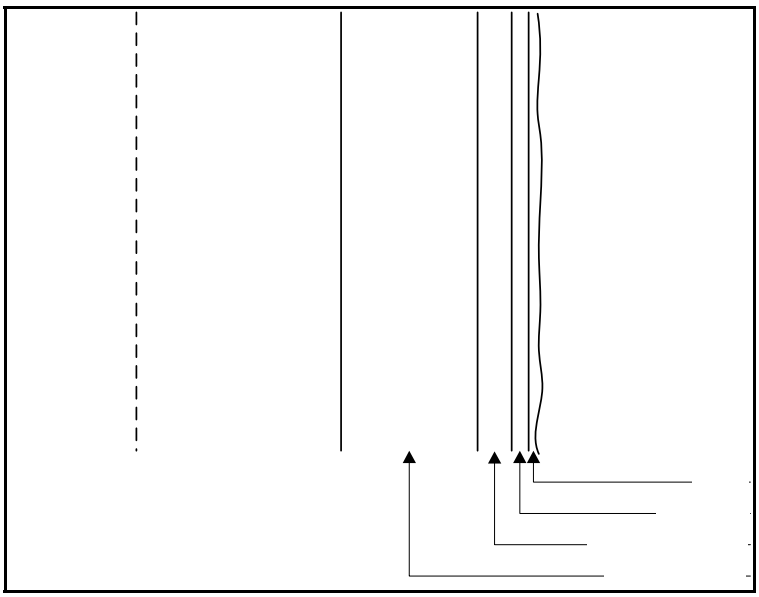

Figure 17 – One-dimensional representation of the region being modelled.

a. Geometry and dimensions

Coordinate system: Cylindrical

Focus dimension: Radial

The radial dimension range and the freeze lining layer dimensions given below are typical values as these are adjusted to suit the objectives of specific experiments.

Dimension ranges:	Dimension	Min.	Max.	Units
	Radial:	0.000	5.000	m
	Axial:	0.000	1.000	m
	Angular:	0.000	2π	radians

Layer dimensions:	Layer	Min.	Max.	Units
	Steel Layer:	4.975	5.000	m
	Ramming Layer:	4.925	4.975	m
	Brick Layer:	4.425	4.925	m
	Freeze lining:	0.000	4.425	m

Standard node size:	Layer	Size	Units
	Steel Layer:	0.00625	m
	Ramming Layer:	0.010	m
	Brick Layer:	0.010	m
	Freeze lining	0.010	m

The dimensions of the freeze lining layer indicate that it reaches from the centre of the furnace to the inner surface of the brick layer. This does not mean that the entire slag bath is solidified, but rather that the entire slag bath can participate in solidification and melting.

The inner position of the freeze lining can be adjusted to be away from the centre of the furnace if the application of the model requires this. Doing this will mean that the entire slag bath will not participate in solidification and melting of the freeze lining. This becomes necessary if a second conductor module (representing the crust on the slag bath, for example) is linked to the same material mixer (in this case the SlagBath).

3.6.5 Heat Transfer

a. Boundary conditions

Because the conductor was divided into four distinct layers, the number of boundary conditions increased from two (for the case where the conductor is viewed as a single layer) to five.

- Steel layer outer surface boundary condition

  Type: Constant temperature (50 °C)

  For details about this boundary condition, see paragraph 3.6.1h Assumption 3.8 on page 38.

- Steel–ramming contact boundary condition

  Type: Contact heat transfer coefficient

The heat transfer coefficient was increased to the maximum value that did not cause numerical instabilities in the FLC model. The reason for this approach is that this contact resistance was assumed not to be rate-determining. For details about this assumption, see paragraph 3.6.1i Assumption 3.9 on page 38.

- Ramming-brick contact boundary condition

  Type: Contact heat transfer coefficient

  The heat transfer coefficient was increased to the maximum value that did not cause numerical instabilities in the FLC model. The reason for this approach is that this contact resistance was assumed not to be rate-determining. For details about this assumption, see paragraph 3.6.1i Assumption 3.9 on page 38.

- Brick-slag contact boundary condition

  Type: Contact heat transfer coefficient

  The heat transfer coefficient was increased to the maximum value that did not cause numerical instabilities in the FLC model. The reason for this approach is that this contact resistance was assumed not to be rate-determining. For details about this assumption, see paragraph 3.6.1i Assumption 3.9 on page 38.

- Freeze lining layer inner surface boundary condition

  Type: Ideal insulation

  No heat transfer was allowed over the inner surface of the freeze lining layer. The first reason was that this layer was sometimes defined to start at the centre of the furnace, which made heat transfer into the inner surface impossible. Secondly, heat is transferred into the freeze lining layer by the bulk exchange of liquid slag with the slag bath. This is discussed in subsequent paragraphs.

b. List of symbols

SYMBOL	DESCRIPTION	UNITS OF MEASURE
$c_{p,material}(T)$	The heat capacity at constant pressure of the material identified by the subscript at temperature T.	kWh/(kg.°C)
ΔH_m^t	The increase (or decrease if negative) of the enthalpy of a finite-difference node identified by m from time step $t-1$ to time step t.	kWh
ΔH_{FEM}^t	The enthalpy change associated with the equilibrium state calculated by the free energy minimiser.	kWh
ΔH_{ref}	The enthalpy of the material at the reference temperature of, in this case, 298.15 K.	kWh/kg
H_m^t	The enthalpy of finite-difference node m at time step t.	kWh
$h_{c,layer1-layer2}$	The contact heat transfer coefficient between the layers identified in the subscript.	kW/(m^2.°C)
$k_{material}(T)$	The thermal conductivity of the material identified by the subscript at temperature T.	kW/(m.°C)
M_{layer}	The number of finite-difference nodes in the layer identified by the subscript.	
M'_{layer}	The index identifying the innermost finite-difference node in the layer identified by the subscript.	

SYMBOL	DESCRIPTION	UNITS OF MEASURE
m	An index identifying a finite-difference node. Nodes are indexed in ascending order as the position (radial, axial or angular) of the node increases.	
$R^t_{m,m'}$	The heat transfer resistance between finite-difference nodes m and m' at time step t.	°C/kW
$R^t_{c,layer1-layer2}$	The contact heat transfer resistance between the two layers identified in the subscript at time step t.	°C/kW
r_m	The radial position of finite-difference node m.	m
Δr_{layer}	The standard radial dimension of finite-difference nodes in the layer identified by the subscript. Innermost and outermost nodes have half this dimension.	m
T^t_m	The temperature of finite-difference node m at time step t.	°C
t	Used as a superscript to indicate the current time step.	
V_m	The volume of finite-difference node m.	m^3
Δz_{layer}	The standard node size of the layer indicated by the subscript.	m
$\Delta z_{\text{freeze lining}}$	The axial dimension of the freeze lining.	m
$\rho_{material}$	The density of the material identified by the subscript.	kg/m^3
$\Delta\tau$	The size of the integration time step of the model.	s

Table 3 – List of symbols used in CHAPTER 3 heat transfer formulation.

c. Steel layer outermost node heat balance

Because this node was treated with a constant-temperature boundary condition, no heat balance was done on it.

d. Layer outermost node heat balance

The equations formulated below are applicable for all layers except the steel layer.

Change in enthalpy = Energy conducted into left face
+ Heat generated within node
– Energy transferred over contact out of right face

$$\Delta H^{t+1}_{M'_L+1} = H^{t+1}_{M'_L+1} - H^t_{M'_L+1} = \frac{T^t_{M'_L+2} - T^t_{M'_L+1}}{R^t_{M'_L+2,M'_L+1}} \cdot \Delta\tau + \Delta H^t_{FEM} - \frac{T^t_{M'_L+1} - T^t_{M'_L}}{R^t_{c,L-L2}} \cdot \Delta\tau$$

$$H^t_{M'_L+1} = \rho_{material} \cdot V_{M'_L+1} \cdot \left[\int_{T_{ref}}^{T^t_{M'_L+1}} c_{p,material}(T)dT + H_{ref} \right]$$

$$V_{M'_L+1} = \pi\left(r^2_{M'_L+1} - \left(r_{M'_L+1} - \frac{\Delta r_L}{2} \right)^2 \right) \cdot \Delta z_{\text{freeze lining}}$$

$$R^t_{M'_L+1,M'_L+2} = \frac{\Delta r_{L2}}{\left(r_{M'_L+1} - \frac{\Delta r_{L2}}{2} \right) \cdot 2\pi \cdot \Delta z_{freezelining} \cdot k_{material}\left(\frac{T^t_{M'_L+1} + T^t_{M'_L+2}}{2} \right)}$$

$$R^t_{c,L-L2} = \frac{1}{r_{M'_L+1} \cdot 2\pi \cdot \Delta z_{\text{freeze lining}} \cdot h_{c,\text{L-L2}}}$$

ΔH^t_{FEM} represents heat associated with solidification and melting as calculated by Gibbs-free-energy minimisation. It is only applicable for *L=FL*.

For the ramming layer: $L = SL$ $L2 = RL$ *material* = Ramming

For the brick layer: $L = RL$ $L2 = BL$ *material* = Magnesia Brick

For the freeze lining: $L = BL$ $L2 = FL$ *material* = Liquid/Solid Slag

e. Layer internal node heat balance

The equations formulated below are applicable to all layers in the model.

Change in enthalpy = Energy conducted into left face
+ Heat generated within node
– Energy conducted out of right face

$$\Delta H_m^{t+1} = H_m^{t+1} - H_m^t = \frac{T_{m+1}^t - T_m^t}{R_{m,m+1}^t} \cdot \Delta\tau + \Delta H_{FEM}^t - \frac{T_m^t - T_{m-1}^t}{R_{m,m-1}^t} \cdot \Delta\tau$$

$$H_m^t = \rho_{material} \cdot V_m \cdot \left[\int_{T_{ref}}^{T_m^t} c_{p,material}(T) dT + H_{ref} \right]$$

$$V_m = \pi\left(\left(r_m + \tfrac{\Delta r_L}{2} \right)^2 - \left(r_m - \tfrac{\Delta r_L}{2} \right)^2 \right) \cdot \Delta z_{\text{freeze lining}}$$

$$R_{m,m+1} = \frac{\Delta r_L}{\left(r_m - \tfrac{\Delta r_L}{2} \right) \cdot 2\pi \cdot \Delta z_{\text{freeze lining}} \cdot k_{\text{material}}\left(\tfrac{T_m^t + T_{m+1}^t}{2} \right)}$$

$$R_{m,m-1} = \frac{\Delta r_L}{\left(r_m + \tfrac{\Delta r_L}{2} \right) \cdot 2\pi \cdot \Delta z_{\text{freeze lining}} \cdot k_{\text{material}}\left(\tfrac{T_m^t + T_{m-1}^t}{2} \right)}$$

ΔH^t_{FEM} represents heat associated with solidification and melting as calculated by Gibbs-free-energy minimisation. It is only applicable for *L=FL*.

For the steel layer: $L = SL$ *material* = Steel $1 < m < M'_{SL}$

For the ramming layer: $L = RL$ *material* = Ramming $M'_{SL} + 1 < m < M'_{RL}$

For the brick layer: $L = BL$ *material* = Magnesia Brick $M'_{RL} + 1 < m < M'_{BL}$

For the freeze lining: $L = FL$ *material* = Solid/Liquid Slag $M'_{BL} + 1 < m < M'_{FL}$

f. Layer innermost node heat balance

The equations formulated below are applicable to all layers except for the freeze lining.

Change in enthalpy = Energy transferred over contact into left face
+ Heat generated within node
– Energy conducted out of right face

$$\Delta H_{M'_L}^{t+1} = H_{M'_L}^{t+1} - H_{M'_L}^{t} = \frac{T_{M'_L+1}^{t} - T_{M'_L}^{t}}{R_{c,L-L2}^{t}} \cdot \Delta\tau + 0 - \frac{T_{M'_L}^{t} - T_{M'_L-1}^{t}}{R_{M'_L,M'_L-1}^{t}} \cdot \Delta\tau$$

$$H_{M'_L}^{t} = \rho_{material} \cdot V_{M'_L} \cdot \left[\int_{T_{ref}}^{T_{M'_L}^{t}} c_{p,material}(T)dT + H_{ref} \right]$$

$$V_{M'_L} = \pi\left(\left(r_{M'_L} + \frac{\Delta r_L}{2} \right)^2 - r_{M'_L}^2 \right) \cdot \Delta z_{freezelining}$$

$$R_{c,L-L2}^{t} = \frac{1}{r_{M'_L} \cdot 2\pi \cdot \Delta z_{freezelining} \cdot h_{c,L-L2}}$$

$$R_{M'_L,M'_L-1}^{t} = \frac{\Delta r_L}{\left(r_{M'_L} + \frac{\Delta r_L}{2} \right) \cdot 2\pi \cdot \Delta z_{freezelining} \cdot k_{material}\left(\frac{T_{M'_L}^{t} + T_{M'_L-1}^{t}}{2} \right)}$$

For the steel layer: $L = SL$ $L2 = RL$ $material$ = Steel

For the ramming layer: $L = RL$ $L2 = BL$ $material$ = Ramming

For the brick layer: $L = BL$ $L2 = FL$ $material$ = Magnesia Brick

g. Freeze lining innermost node heat balance

This node was treated with an ideal insulation boundary condition on its inner surface. This was done to simplify the model. It means that the model will stop receiving heat from the slag bath once this innermost node has become completely solid.

The radial dimension of the freeze lining layer was chosen in such a way that this never happened. This constraint of the model was therefore avoided by appropriate use of the model.

Change in enthalpy = Energy transferred into left face
+ Heat generated within node
– Energy conducted out of right face

$$\Delta H_{M'_L}^{t+1} = H_{M'_L}^{t+1} - H_{M'_L}^{t} = 0 + \Delta H_{FEM}^{t} - \frac{T_{M'_L}^{t} - T_{M'_L-1}^{t}}{R_{M'_L,M'_L-1}^{t}} \cdot \Delta\tau$$

$$H_{M'_L}^{t} = \rho_{material} \cdot V_{M'_L} \cdot \left[\int_{T_{ref}}^{T_{M'_L}^{t}} c_{p,material}(T)dT + H_{ref} \right]$$

$$V_{M'_L} = \pi\left(\left(r_{M'_L} + \frac{\Delta r_L}{2} \right)^2 - r_{M'_L}^2 \right) \cdot \Delta z_{freezelining}$$

$$R_{M'_L,M'_L-1}^{t} = \frac{\Delta r_L}{\left(r_{M'_L} + \frac{\Delta r_L}{2} \right) \cdot 2\pi \cdot \Delta z_{freezelining} \cdot k_{material}\left(\frac{T_{M'_L}^{t} + T_{M'_L-1}^{t}}{2} \right)}$$

ΔH^t_{FEM} represents heat associated with solidification and melting as calculated by Gibbs-free-energy minimisation.

For this layer: $L = FL \quad material = \text{Liquid/Solid Slag}$

h. Liquid slag effective thermal conductivity

Because of mixing in the slag bath, the effective thermal conductivity of the liquid slag is higher than the 0.001 kW/(m.°C) that was assumed previously for the solid slag (Assumption 3.6, page 37). The convective heat transfer from the slag bath (and therefore the higher effective thermal conductivity) was accounted for by assigning a higher thermal conductivity value to liquid slag, calculating a single temperature for the entire slag bath at each time step, and then bringing this slag into contact with the freeze lining at its surface. The end result was that virtually no temperature gradient was created in the liquid slag adjacent to the freeze lining.

The influence of effective thermal conductivity was tested during validation of the FLC model. It was not found to have a major influence on modelling results. The effective thermal conductivity that was finally used was 5 times that of the solid slag. This is similar to what has been assumed for liquid metal in the molten core of continuous casting strands (Brimacombe, 1976).

3.6.6 Slag Solidification and Melting

Equilibrium solidification and melting of slag was modelled by using a Gibbs-free-energy-minimisation technique. The Gibbs-free-energy minimiser calculates the most stable combination of phases and phase constituents from the material and enthalpy provided as inputs. The ChemApp library (GTT Technologies, 2001) was used for this purpose.

3.7 MODEL SOLUTION

3.7.1 Flow Sheet

Since the FLC model used the slag bath only as a boundary condition, and the slag bath and its modelling were not included, the FLC model could not be used on its own. It formed part of a larger modelling framework and always had to be incorporated into a larger model that was able to calculate the slag bath state. The modelling framework used for the construction of these models, is the one developed by Pauw (1989). A simple example is given in Figure 18. The remaining discussions about the FLC model will be done within the context of the model presented in Figure 18.

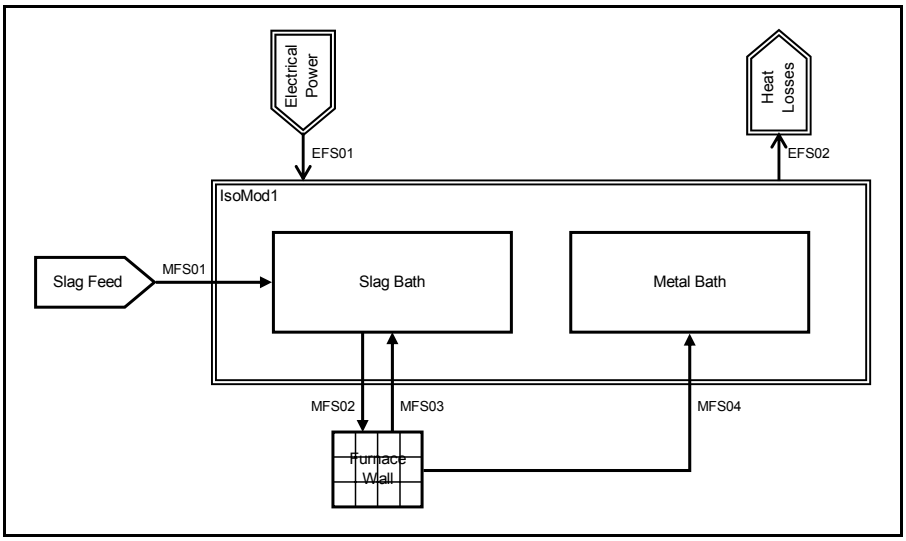

Figure 18 – Flow sheet of a simple process model incorporating the FLC model.

See APPENDIX B for a description of the various model elements.

The elements of the flow sheet presented in Figure 18 are as follows:

- SlagFeed

  The SlagFeed material input module delivers liquid slag that is poured into the SlagBath mixer to establish an initial condition. The material produced by the SlagFeed material input module is discharged into the MFS01 material flow stream.

- MFS01

  The MFS01 material flow stream connects the SlagFeed material input module with the SlagBath mixer. It assists in establishing an initial condition.

- SlagBath

  The SlagBath mixer contains all liquid slag in the system.

- MFS02

  The MFS02 material flow stream connects the SlagBath mixer with the Furnace Wall conductor. It transports material that is about to participate in solidification and melting to the freeze lining.

- FurnaceWall

  The FurnaceWall conductor contains the 4-layer FLC conductor model that is the focus of this chapter.

- MFS03

  The MFS03 material flow stream connects the FurnaceWall conductor with the SlagBath mixer. It transports material that participated in solidification and melting from the freeze lining.

- MFS04

  The MFS04 material flow stream connects the FurnaceWall conductor with the MetalBath mixer. It transports liquid metal that may form as a result of solidification and melting at the freeze lining inner surface.

- MetalBath

  The MetalBath mixer contains all liquid metal in the system.

- ElectricalPower

  The ElectricalPower energy input module delivers electrical energy and represents a furnace electrical system.

- EFS01

  The EFS01 energy flow stream connects the ElectricalPower energy input module with the IsoMod1 isothermal module. In this simplified case, all energy from ElectricalPower reaches IsoMod1.

- IsoMod1

  The IsoMod1 isothermal module represents the slag and metal baths as an isothermal zone.

- EFS02

  The EFS02 energy flow stream connects the IsoMod1 isothermal module with the HeatLosses energy output module. All heat that is lost from the SlagBath and Metal Bath mixers by means other than conduction through the FurnaceWall conductor leaves IsoMod1 through EFS02.

- HeatLosses

  The HeatLosses energy output module represents all heat losses from the SlagBath and Metal Bath mixers other than the losses through the FurnaceWall conductor.

3.7.2 Initial Conditions

Before the step-by-step solution of the model was started, it was set up with the following initial conditions:

- The Steel Layer was set up with all nodes being filled with Steel, and with a predetermined temperature for each node. The outermost node temperature was set equal to the constant temperature boundary condition and the other nodes equal to values that were determined not to cause instabilities when the model was started. These temperatures were close to the values that the nodes would converge to.

- The Ramming Layer was handled identically to the Steel Layer, except for its outermost node. This node temperature was also predetermined in such a way that it did not cause instabilities when the model was started.

- The Brick Layer was handled identically to the Ramming Layer.

- The Freeze Lining Layer was handled in the same way as the Ramming Layer, except that this layer was only partially filled with solid slag. The nodes containing solid slag were assigned initial

temperatures. The composition of the solid slag used to fill the slag was the same as the first product that would solidify from the liquid slag bath.

3.7.3 Solution

The following procedure was used to solve the model during each time step:

- Fill the Freeze Lining layer void with material from the SlagBath. The void refers to those nodes that do not contain any material. Upon start-up, this includes all freeze lining nodes except those nodes and part of nodes that were filled as part of the initial conditions. Step (a) of Figure 19 shows the condition before filling the void, and step (b) the condition after filling the void.
- For each layer L:
    - Calculate the enthalpy change for each node of L due to heat transfer and calculate the new temperature for each node of L. The result of this is indicated as step (c) of Figure 19. The temperature profile is now different.
    - If L is the Freeze Lining layer:
        - Combine all liquid slag in the layer with a layer of solid slag. The result is shown in step (d) of Figure 19.
        - Calculate the equilibrium state of the combined material by Gibbs-free-energy minimisation. The result is shown in step (e) of Figure 19. More solid slag is now present and the combined material is isothermal.
        - Should any solid material result from the equilibrium calculation, this material is assigned to the outermost node m that is partially or completely void first, then to its inner neighbour $m+1$, then to $m+2$, etc. The result is shown in step (f) of Figure 19. A complete thermal profile has been applied to the solid slag layer.
        - Once the solid material has been distributed, the liquid resulting from the equilibrium calculation is used to fill the remaining empty or partially empty nodes. The result is shown in step (f) of Figure 19.
- Drain all liquid slag from the freeze lining and add it back to the SlagBath mixer. The result is shown in step (g) of Figure 19.
- Drain all liquid metal from the freeze lining and add it to the Metal Bath mixer. For the sake of simplicity this is not indicated on Figure 19.
- Calculate new liquid slag composition and IsoMod1 temperature for the current time step (t).
  This is not part of the FLC model since the slag bath is simply used as a boundary condition. It is done by other modules (SlagBath and IsoMod1) in the flow sheet.

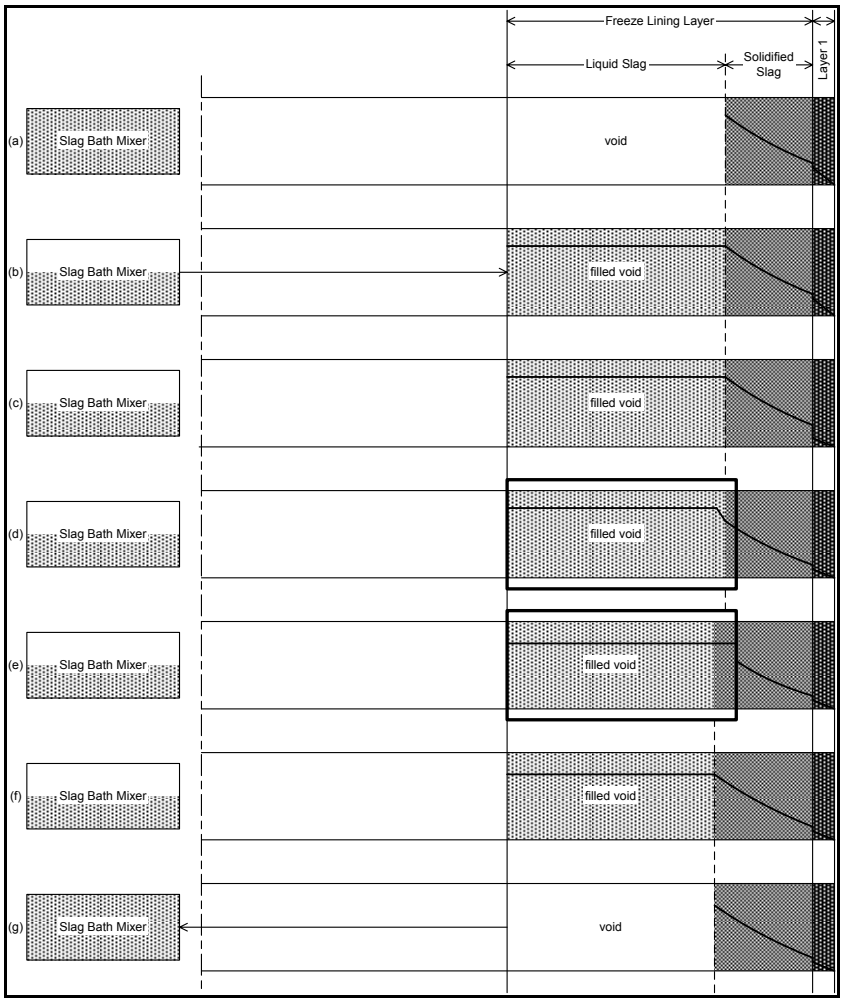

Figure 19 – Schematic representation of steps in the FLC model solution procedure.

3.8 MODEL VALIDATION

3.8.1 Purpose

The purpose of validation is to confirm the numerical integrity of the FLC model (Thomas and Brimacombe, 1997).

3.8.2 Objectives

Model validation had to achieve the following objectives:

- Confirm the integrity of the heat transfer calculations.
- Confirm that the combination of the ChemApp Gibbs-free-energy-minimisation routine and the thermochemical data files used by the model calculated realistic equilibrium results.
- Confirm that the model was able to describe solidification and melting of the freeze lining.

3.8.3 Methodology

The heat transfer calculations included in the model were validated by checking steady state results generated by the model against a set of analytically calculated steady state results. Example results of the analytical calculation are shown in Figure 20 and Figure 21. From Figure 21 it is clear that the freeze lining generally represents the largest thermal resistance since the steepest fall in temperature occurs in this layer.

The model was initialised with a steady state heat flow rate of 300 kW into the system and through the wall. The input heat flow rate was changed to a new value of either 250 kW or 350 kW. The model was then left to reach a new steady state. The temperatures calculated by the model were then compared with a corresponding analytical solution.

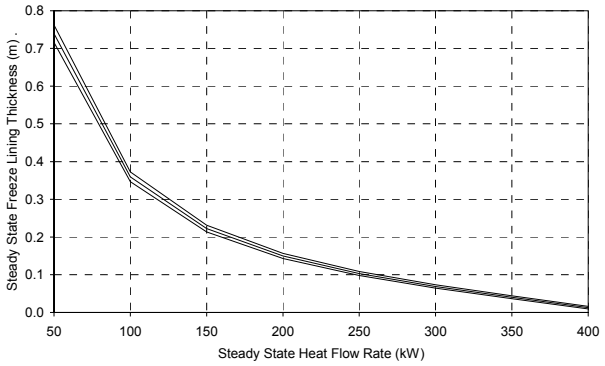

Figure 20 – Analytically calculated steady state freeze lining thickness vs. heat flow rate.
The bottom line represents a slag with a liquidus temperature of 1550 °C, the middle line 1600 °C and the top line 1650 °C.

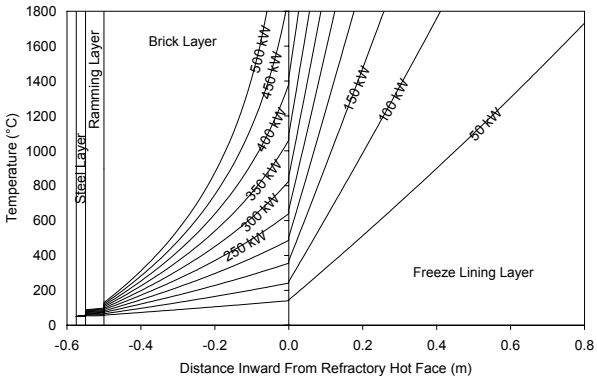

Figure 21 – Analytically calculated steady state temperature profiles.

The ChemApp Gibbs-free-energy-minimisation routine and thermochemical data files were used to generate results that were subsequently compared with results of the same calculations done by FactSage 5.2. Since FactSage contains critically evaluated data of the thermochemical system under consideration, it was believed to be a trustworthy reference. The agreement between the ChemApp and FactSage results was found to be good. This was expected because the ChemApp data file was most probably generated using FactSage 5.2. Details of these comparisons are not presented here.

The results generated by the comparison between model results and analytically calculated results were used to achieve the last validation objective. Because a change in input heat flow rate caused the freeze lining to either become thicker in the case of a reduced input heat flow rate, or thinner in the case of an increased input heat flow rate, these experiments demonstrated whether or not the model was able to describe solidification and melting of the freeze lining.

3.8.4 Validation Experiments

a. Experiment 3.1

Objective: Confirm the integrity of the model's heat transfer equations, and that the model is able to describe solidification and melting of the freeze lining.

Initial condition: The SlagBath was filled with a 10%-60%-30% (FeO-TiO_2-Ti_2O_3 mass percentages) slag at a temperature of 1633 °C. This temperature is close to the liquidus temperature of the slag. The slag composition was chosen to be on the rutile side of the eutectic groove. This meant that rutile was the primary phase that solidified.

The conductivity of the liquid slag was set equal to 0.001 kW/(m.°C), the same as the solid slag.

The freeze lining thickness and the temperature distribution through the freeze lining, brick, ramming and steel were initialised as close as possible to an analytically calculated steady state for a heat flow rate of 300 kW.

Steps: The model was allowed to run until the freeze lining thickness and the temperature distribution through the freeze lining, brick, ramming and steel reached steady state values at 300 kW. This result is referred to as the '300 kW Base Condition'.

With the 300 kW Base Condition as starting point, the input heat flow rate via the ElectricalPower energy input module was then set equal to 250 kW, and the model was allowed to reach a new steady state.

The 300 kW Base Condition was subsequently again used as starting point, the input heat flow rate via the ElectricalPower energy input module was next set equal to 350 kW, and the model was allowed to reach a new steady state.

b. Experiment 3.2

Objective: Confirm the integrity of the model's heat transfer equations, and that the model is able to describe solidification and melting of the freeze lining.

Determine the influence of an increase in effective thermal conductivity of the liquid slag.

Initial condition: As for Experiment 3.1, but with a liquid slag conductivity of 0.005 kW/(m.°C).

Steps: As for Experiment 3.1.

c. Experiment 3.3

Objective: Confirm the integrity of the model's heat transfer equations, and that the model is able to describe solidification and melting of the freeze lining.

Initial condition: As for Experiment 3.1, but with a slag composition of 10%-50%-40% (FeO-TiO_2-Ti_2O_3 mass percentages) and a temperature of 1617 °C.

Steps: As for Experiment 3.1.

d. Experiment 3.4

Objective: Confirm the integrity of the model's heat transfer equations, and that the model is able to describe solidification and melting of the freeze lining.

Determine the influence of an increase in effective thermal conductivity of the liquid slag.

Initial condition: As for Experiment 3.3, but with a liquid slag conductivity of 0.005 kW/(m.°C).

Steps: As for Experiment 3.1.

e. Experiment 3.5

Objective: Confirm the integrity of the model's heat transfer equations, and that the model is able to describe solidification and melting of the freeze lining.

Determine the influence of an increase in effective thermal conductivity of the liquid slag.

Initial condition: As for Experiment 3.3, but with a liquid slag conductivity of 0.010 kW/(m.°C).

Steps: As for Experiment 3.1.

f. Experiment 3.6

Objective: Confirm the integrity of the model's heat transfer equations, and that the model is able to describe solidification and melting of the freeze lining.

Determine the influence of an increase in effective thermal conductivity of the liquid slag.

Initial condition: As for Experiment 3.1, but with a slag composition of 15%-55%-30% (FeO-TiO_2-Ti_2O_3 mass percentages), a temperature of 1587 °C and a liquid slag conductivity of 0.005 kW/(m.°C).

Steps: As for Experiment 3.1.

3.8.5 Validation Results

Results of the validation experiments are presented below in the form of two graphs per experiment step. The graph on the left-hand side shows a comparison between an analytically calculated steady-state temperature profile of the furnace wall and freeze lining (solid line), and the same profile calculated by the FLC model (crosses).

The second graph shows the difference between temperatures calculated by the FLC model and analytically calculated temperature values. Positive values indicate overestimation by the FLC model.

The reference point (zero) of the radial position is the centre of the furnace.

a. Experiment 3.1

%FeO	$\%TiO_2$	$\%Ti_2O_3$	$k_{liquid\ slag}$
10	60	30	0.001 kW/(m.°C)

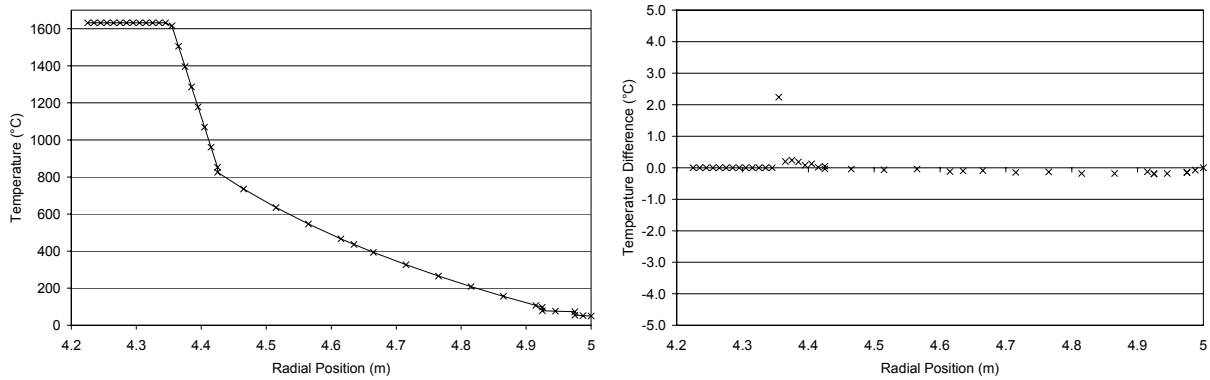

Figure 22 – Validation experiment 3.1 results for a heat flow rate of 300 kW (the 300kW Base Condition).

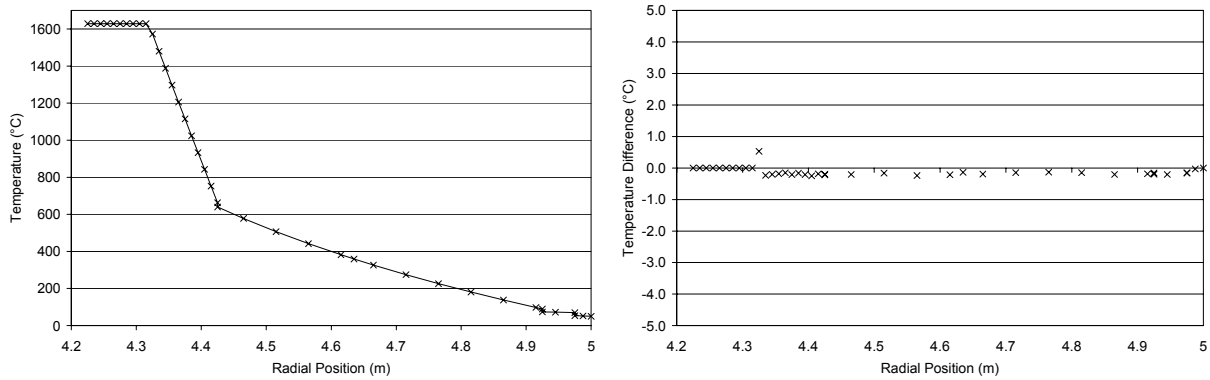

Figure 23 – Validation experiment 3.1 results for a heat flow rate of 250 kW.

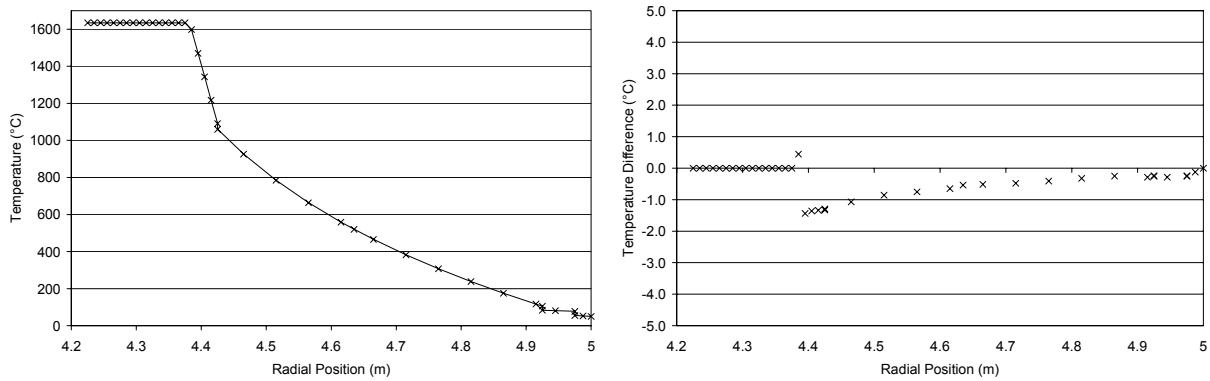

Figure 24 – Validation experiment 3.1 results for a heat flow rate of 350 kW.

b. Experiment 3.2

%FeO	%TiO_2	%Ti_2O_3	$k_{liquid\ slag}$
10	60	30	0.005 kW/(m.°C)

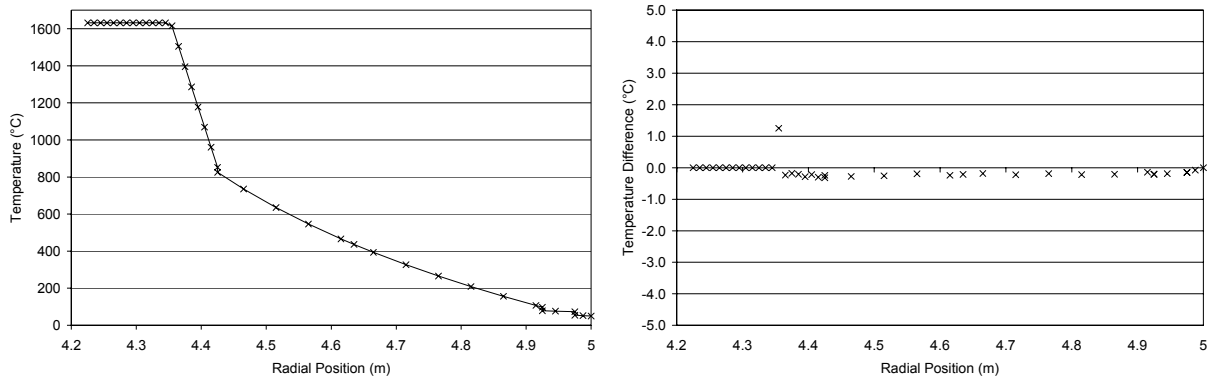

Figure 25 – Validation experiment 3.2 results for a heat flow rate of 300 kW (the 300kW Base Condition).

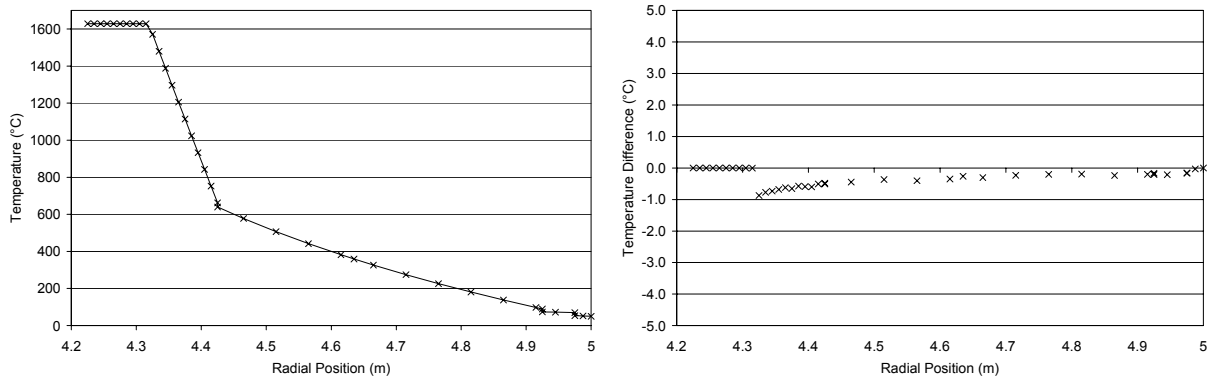

Figure 26 – Validation experiment 3.2 results for a heat flow rate of 250 kW.

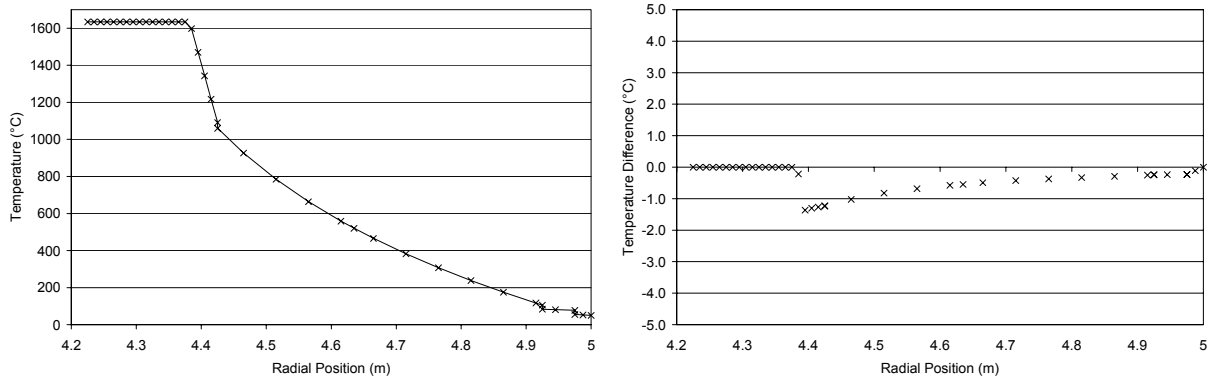

Figure 27 – Validation experiment 3.2 results for a heat flow rate of 350 kW.

c. Experiment 3.3

%FeO	%TiO_2	%Ti_2O_3	$k_{liquid\ slag}$
10	50	40	0.001 kW/(m.°C)

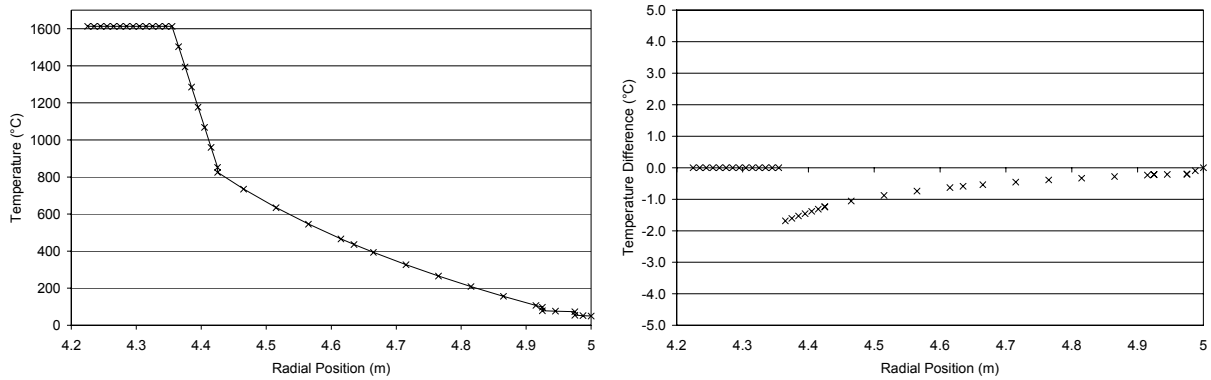

Figure 28 – Validation experiment 3.3 results for a heat flow rate of 300 kW (the 300kW Base Condition).

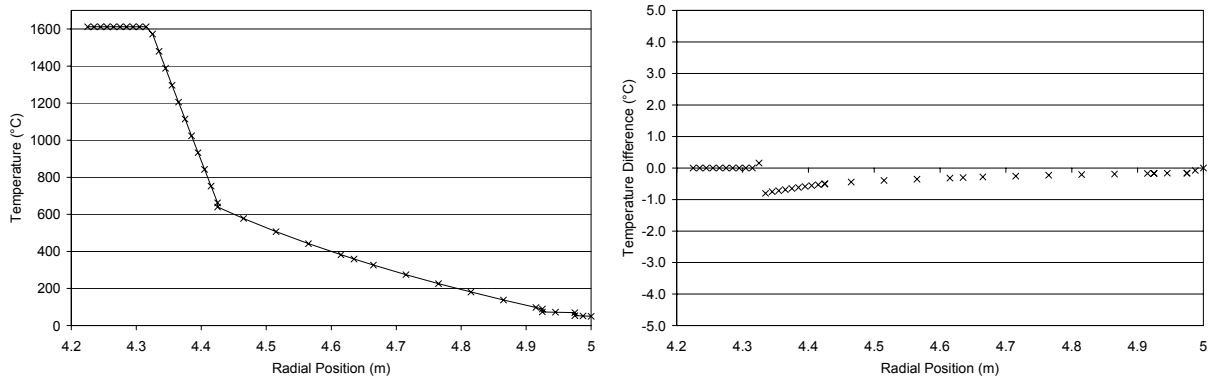

Figure 29 – Validation experiment 3.3 results for a heat flow rate of 250 kW.

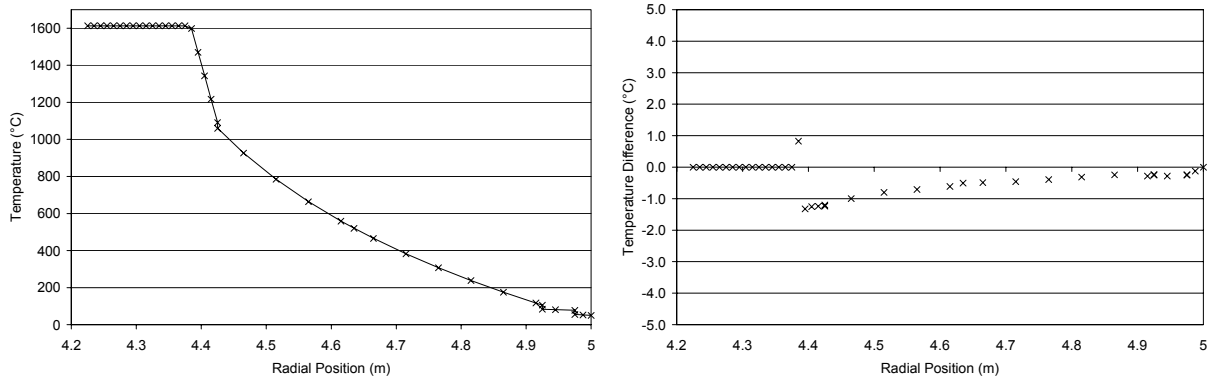

Figure 30 – Validation experiment 3.3 results for a heat flow rate of 350 kW.

d. Experiment 3.4

%FeO	%TiO_2	%Ti_2O_3	$k_{liquid\ slag}$
10	50	40	0.005 kW/(m.°C)

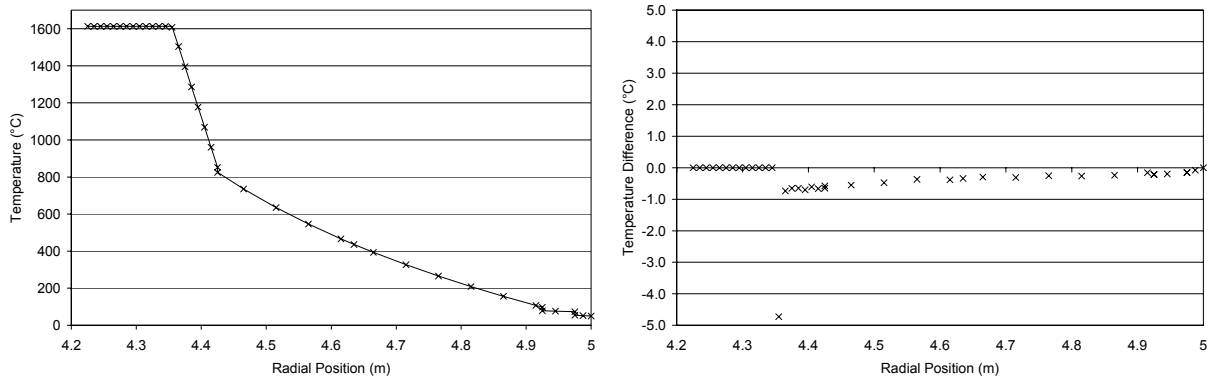

Figure 31 – Validation experiment 3.4 results for a heat flow rate of 300 kW (the 300kW Base Condition).

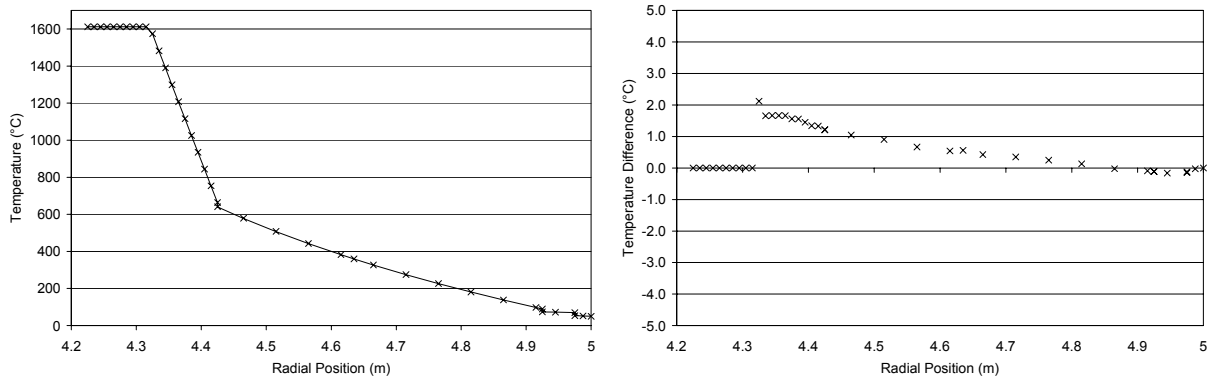

Figure 32 – Validation experiment 3.4 results for a heat flow rate of 250 kW.

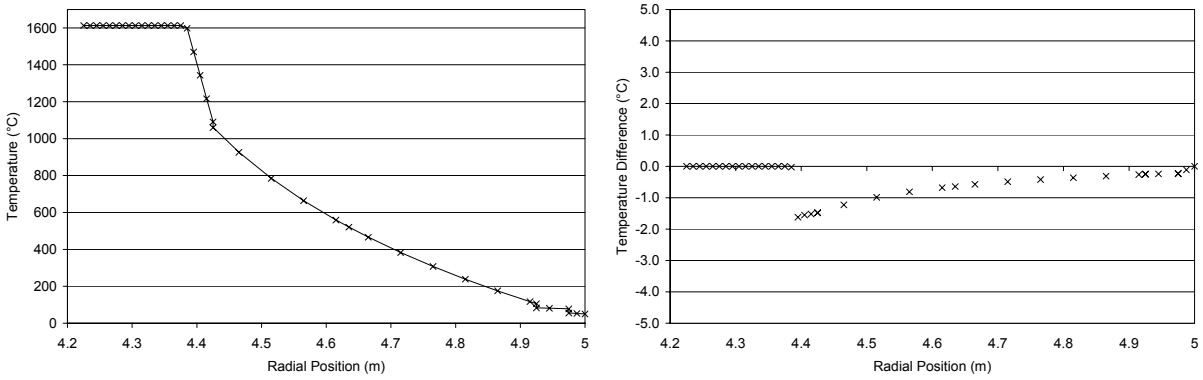

Figure 33 – Validation experiment 3.4 results for a heat flow rate of 350 kW.

e. Experiment 3.5

%FeO	$\%TiO_2$	$\%Ti_2O_3$	$k_{liquid\ slag}$
10	50	40	0.010 kW/(m.°C)

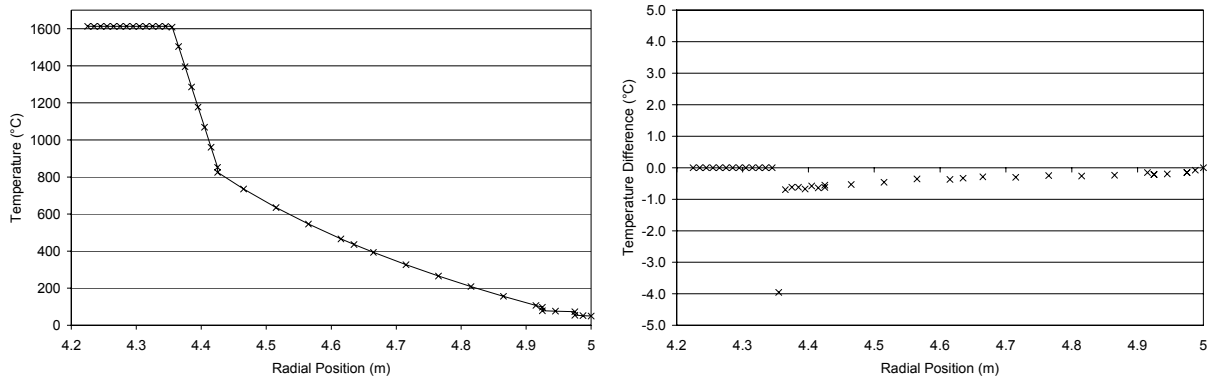

Figure 34 – Validation experiment 3.5 results for a heat flow rate of 300 kW.

f. Experiment 3.6

%FeO	%TiO_2	%Ti_2O_3	$k_{liquid\ slag}$
15	55	30	0.005 kW/(m.°C)

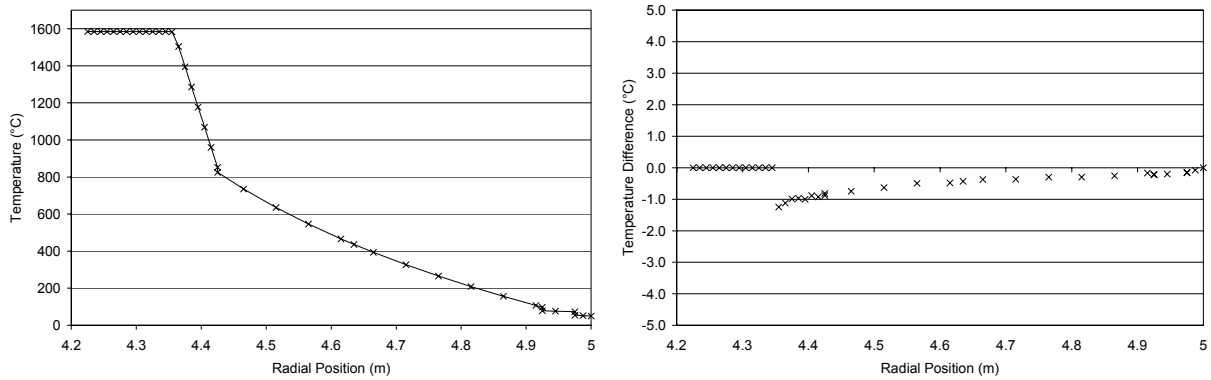

Figure 35 – Validation experiment 3.6 results for a heat flow rate of 300 kW (the 300kW Base Condition).

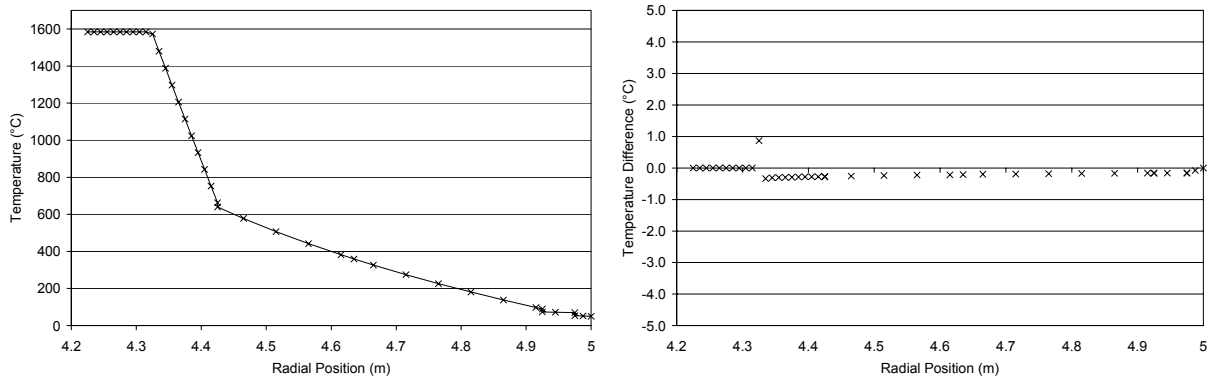

Figure 36 – Validation experiment 3.6 results for a heat flow rate of 250 kW.

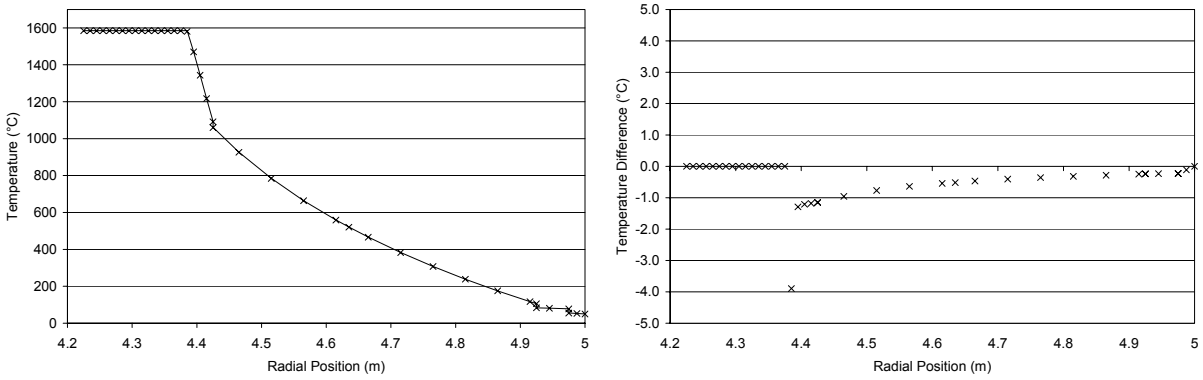

Figure 37 – Validation experiment 3.6 results for a heat flow rate of 350 kW.

g. Summary

A relatively wide range of conditions were covered by the validation experiments listed above. The model was able to reach steady state values that never deviated by more than 5 °C from the analytical solution. The deviations were believed to be due to round-off errors due to the ever-decreasing enthalpy change of the nodes as steady state is approached.

The variation in effective thermal conductivity between the various experiments did not appear to have a large influence. A figure of 0.005 kW/(m.°C) was finally decided on for use during subsequent work.

3.9 COMPARISON WITH ACTUAL DATA

Due to the confidentiality of most information pertaining to the industrial process, no comparison with actual data could be published here. The comparisons against analytically calculated values therefore serve as the only validation of the FLC model.